PROCEEDINGS OF SCIENCE

MS-TP-25-5, JLAB-THY-25-4211

O(a) improvement of the flavour singlet scalar density in a setup with Wilson fermions

Pia Leonie Jones Petrak,[a,b,*] **Jochen Heitger**[b] **and Fabian Joswig**[b,c]

[a] *Theory Center, Jefferson Lab, Newport News, Virginia 23606, USA*

[b] *Institut für Theoretische Physik, Universität Münster, Wilhelm-Klemm-Straße 9, 48149 Münster, Germany*

[c] *School of Physics and Astronomy, University of Edinburgh, Edinburgh EH9 3JZ, United Kingdom*

E-mail: pialjp@jlab.org, heitger@uni-muenster.de

We report on our Ward identity determination of the O(a) improvement coefficient for the flavour singlet scalar density, namely $g_{\rm S}$, from three-flavour lattice QCD with Wilson-clover fermions and the tree-level Symanzik improved gauge action. We employ five couplings, $g_0^2 \in [1.5, 1.77]$, that cover the range used in large-volume CLS simulations. While $g_{\rm S}$ itself is for instance relevant for the O(a) improvement of meson and baryon sigma terms, a relation to $b_{\rm g}$, the O(a) improvement parameter of the gauge coupling, can also be established, allowing for its non-perturbative extraction as well. With Wilson fermions, $b_{\rm g}$ is in principle required for full O(a) improvement at non-vanishing sea quark masses. We outline our procedure for extracting $b_{\rm g}$.

The 41st International Symposium on Lattice Field Theory (LATTICE2024)
28 July - 3 August 2024
Liverpool, UK

*Speaker

PoS(LATTICE2024)290

1. Introduction

The O(a) improvement parameter of the flavour singlet scalar density, termed $g_{\rm S}$, is for instance relevant for the full O(a) improvement of meson and baryon sigma terms, $\sigma_q = m_q \langle H|\bar{q}q|H\rangle$, in a setup with Wilson fermions, see [1]. The flavour singlet scalar density $\bar{q}q$ of flavour q enters in the matrix element that is multiplied by the quark mass m_q. $|H\rangle$ refers to the ground state of a hadron H. So far $g_{\rm S}$ is only known from perturbation theory, see eq. (3) below; as it is expected to be small it has been neglected in all sigma term calculations, as reported in [2, 3]. In [4] its impact is estimated from perturbation theory to be of the order of -0.05 MeV on their estimate of the pion-nucleon sigma term of $\sigma_\pi^{\rm N} = (43.6 \pm 3.8)$ MeV. Thus in this case perturbation theory indeed indicates that $g_{\rm S}$ can be neglected since its effect is smaller than the uncertainty's.

However, for a more reliable estimation, a non-perturbative study of $g_{\rm S}$ is crucial and becoming more relevant as the precision of sigma term computations increases. The aim of our work is to perform a non-perturbative determination in the range of the CLS couplings, $g_0^2 \in [1.5, 1.77]$.

Furthermore, the $g_{\rm S}$ estimates may be used to obtain $b_{\rm g}$ via the relation [1]

$$b_{\rm g} = 2 g_0^2 g_{\rm S} \,. \tag{1}$$

In a setup with Wilson fermions the O(a) improvement parameter of the gauge coupling, $b_{\rm g}$, is in principle required for full O(a) improvement at non-vanishing sea quark masses as $\tilde{g}_0^2 = g_0^2 \cdot (1 + a b_g(g_0^2) {\rm Tr} M_{\rm q}/N_{\rm f})$ [1], where $M_{\rm q}$ denotes the sea quark mass matrix. For the action and coupling range employed here, $b_{\rm g}$ is only known from one-loop perturbation theory [5, 6] as

$$b_{\rm g} = 0.012000(2) \times N_{\rm f}\, g_0^2 + {\rm O}\big(g_0^4\big) \,. \tag{2}$$

For a lower range of couplings, $g_0^2 \in [0.4, 1.5]$, there has been a recent non-perturbative determination [7] relevant for ALPHA's decoupling strategy to determine the strong coupling [8]. Our determination will be relevant for calculations using the CLS ensembles (see [9]) such as sigma term determinations or other computations in the range of the CLS couplings with Wilson fermions.

By inserting eq. (2) for $b_{\rm g}$ in eq. (1) we retrieve a lowest-order perturbative prediction for $g_{\rm S}$,

$$g_{\rm S} = 0.012000(2) \times N_{\rm f}/2 + {\rm O}\big(g_0^2\big) \,. \tag{3}$$

Note that this work's non-perturbative $g_{\rm S}$ results cannot be used to extract $b_{\rm g}$ via eq. (1) and hence, cannot be directly compared to the above perturbative expression: an additional term needs to be included in the $g_{\rm S}$ Ward identity, used here, for the relation from eq. (1) to hold, see sect. (5). There, we also detail the next steps necessary to obtain the adequate $g_{\rm S}$ estimates as to extract $b_{\rm g}$ via eq. (1).

2. Chiral Ward Identities

The well-known PCAC relation is derived from the general continuum axial Ward identity

$$\int_{\mathcal{R}} {\rm d}^4x\, \epsilon^a(x) \left[\partial_\mu \left\langle A_\mu^a(x) O\right\rangle - 2m \left\langle P^a(x) O\right\rangle\right] = -\left\langle \delta_{\rm A} O\right\rangle \tag{4}$$

by choosing the operator O to be an exterior single operator $O_{\rm ext}$, i.e. located outside the region R such that its axial variation is zero, $\langle \delta_{\rm A} O\rangle = \langle \delta_{\rm A} O_{\rm ext}\rangle = 0$. Also, we always impose $\epsilon^a(x) = \epsilon =$

const. for the smallness parameter so that the Ward identity reflects global chiral symmetry. A^a_μ, P^a and m denote the axial current, pseudo-scalar density and degenerate quark mass, respectively. Here, we derive a Ward identity suggested in [1], see [10] for an earlier account of similar identities.

We consider a singlet composite operator $O = S^0 O_{\text{ext}}$ where the flavour singlet scalar density is defined by $S^0(x) = \mathrm{i}\bar{\psi}(x)T^0\psi(x)\,, T^0 = -\mathrm{i}/\sqrt{2N_\mathrm{f}}\mathbb{1}_{N_\mathrm{f}\times N_\mathrm{f}}$ in the $SU(N_\mathrm{f})$ flavour basis. The diagonal flavour matrix T^0 is introduced to handle flavour singlet quantities such as this one. With O_{ext} lying outside R, we have $\langle \delta_A O\rangle = \langle [\delta_A S^0(y)] O_{\text{ext}}\rangle$ and obtain

$$\delta_A S^0(y) = \frac{\mathrm{i}}{\sqrt{2N_\mathrm{f}}}\left[\delta_A\bar{\psi}(y)\psi(y) + \bar{\psi}(y)\delta_A\psi(y)\right] = -\sqrt{\frac{2}{N_\mathrm{f}}}\epsilon^a(y)P^a(y) \tag{5}$$

for the current under small axial variations $\epsilon^a(x)$ of the action. Inserting our choice of operator in eq. (4) and following the same notation and procedure as in [11] (for a non-singlet Ward identity to obtain the parameter Z, defined below eq. (9)), we transfer the Ward identity to the lattice:

$$Z_\mathrm{A} Z^0_\mathrm{S} a^6 \sum_{\mathbf{x},\mathbf{y}} \langle \left[A^a_0(t_2;\mathbf{x}) - A^a_0(t_1;\mathbf{x})\right] S^0(y) O^a\rangle \tag{6a}$$

$$-2am Z_\mathrm{A} Z^0_\mathrm{S} a^6 \sum_{\mathbf{x},\mathbf{y}} \sum_{x_0=t_1}^{t_2} \omega(x_0)\langle P^a(x) S^0(y) O^a\rangle \tag{6b}$$

$$= -\sqrt{\frac{2}{N_\mathrm{f}}} Z_\mathrm{P} a^3 \sum_{\mathbf{y}} \langle P^a(y) O^a\rangle \tag{6c}$$

where the external source was set to $O_{\text{ext}} = O^a$ as defined in [11] and Z_A, Z^0_S and Z_P are the renormalisation parameters. The weight factor $\omega(x_0)$ is needed to implement the trapezoidal rule for discretising integrals. Repeated flavour indices a are summed over and m is the PCAC mass.

We also consider another choice of operator for O in eq. (4), $O = \mathbb{1} O_{\text{ext}} = \mathbb{1} O^a$. The Ward identity can be derived in the same fashion leading to

$$Z_\mathrm{A} Z^0_\mathrm{S} a^6 \sum_{\mathbf{x},\mathbf{y}} \langle \left[A^a_0(t_2;\mathbf{x}) - A^a_0(t_1;\mathbf{x})\right] O^a\rangle\langle S^0(y)\rangle \tag{7a}$$

$$-2am Z_\mathrm{A} Z^0_\mathrm{S} a^6 \sum_{\mathbf{x},\mathbf{y}} \sum_{x_0=t_1}^{t_2} \omega(x_0)\langle P^a(x) O^a\rangle\langle S^0(y)\rangle \tag{7b}$$

$$= 0 \tag{7c}$$

The main difference is that the r.h.s. of eq. (4) is zero in this case as $\langle \delta_A O\rangle = \langle [\delta_A \mathbb{1}] O_{\text{ext}}\rangle + \langle \mathbb{1}[\delta_A O_{\text{ext}}]\rangle = 0$: the flavour variation of the constant unity matrix is clearly zero (while the variation is generally zero outside R where O_{ext} is again defined).

Now it will become clearer why these two Ward identities (6) and (7) are of use. Having inserted the improvement pattern for all operators, a divergence cancels when the two equations are subtracted. The (cubic) divergence lies in the $e_\mathrm{S}(g_0^2)$ term in the improvement pattern of the flavour singlet scalar density [10] (see [1] for a notation more similar to the one applied here),

$$(S_\mathrm{I})^0(x) = S^0(x) + \frac{1}{\sqrt{2N_\mathrm{f}}} a^{-3} e_\mathrm{S}(g_0^2)\mathbb{1} + \frac{1}{\sqrt{2N_\mathrm{f}}} a g_\mathrm{S}(g_0^2)\widetilde{\mathrm{Tr}}[F_{\mu\nu}(x)F_{\mu\nu}(x)] + \mathrm{O}(a^2)\,, \tag{8}$$

where $\widetilde{\mathrm{Tr}}$ stands for the trace over colour indices. Note that the discretised form of the field strength, $\widetilde{\mathrm{Tr}}[F_{\mu\nu}(x)F_{\mu\nu}(x)]$, must be local, symmetric w.r.t. the site where the bilinear S^0 is placed and based on the gauge action employed, see [1]. We write this discretised form as $\{\widetilde{\mathrm{Tr}}[FF](x)\}^{S_\mathrm{g}}$.

We apply the improvement scheme to S^0 in both Ward identities (6) & (7) and subtract the now O(a) improved Ward identities from one another as to make use of the fact that $\langle a^{-3} e_{\rm S}(g_0^2) \mathbb{1} O\rangle = \langle a^{-3} e_{\rm S}(g_0^2)\mathbb{1}\rangle\langle O\rangle$. So all terms containing $e_{\rm S}(g_0^2)$ are the same in both equations and cancel. The combined Ward identity simplifies to

$$a^6 \sum_{x,\mathbf{y}} (\delta_{x_0,t_2} - \delta_{x_0,t_1}) \Big\{ \Big[\big\langle A_0^a(x) S^0(y) O^a \big\rangle - \big\langle A_0^a(x) O^a \big\rangle \big\langle S^0(y) \big\rangle \Big] \tag{9a}$$

$$+ \frac{a g_{\rm S}}{\sqrt{2N_{\rm f}}} \Big[\big\langle A_0^a(x) \{\widetilde{\rm Tr}[FF](y)\}^{S_{\rm g}} O^a \big\rangle - \big\langle A_0^a(x) O^a \big\rangle \big\langle \{\widetilde{\rm Tr}[FF](y)\}^{S_{\rm g}} \big\rangle \Big] \tag{9b}$$

$$+ a c_{\rm A} \partial x_0 \Big[\big\langle P^a(x) S^0(y) O^a \big\rangle - \big\langle P^a(x) O^a \big\rangle \big\langle S^0(y) \big\rangle \Big] \Big\} \tag{9c}$$

$$- a^6 \sum_{\mathbf{x},\mathbf{y}} 2am \sum_{x_0=t_1}^{t_2} \omega(x_0) \Big\{ \Big[\big\langle P^a(x) S^0(y) O^a \big\rangle - \big\langle P^a(x) O^a \big\rangle \big\langle S^0(y) \big\rangle \Big] \tag{9d}$$

$$+ \frac{a g_{\rm S}}{\sqrt{2N_{\rm f}}} \Big[\big\langle P^a(x) \{\widetilde{\rm Tr}[FF](y)\}^{S_{\rm g}} O^a \big\rangle - \big\langle P^a(x) O^a \big\rangle \big\langle \{\widetilde{\rm Tr}[FF](y)\}^{S_{\rm g}} \big\rangle \Big] \Big\} \tag{9e}$$

$$= -\sqrt{\frac{2}{N_{\rm f}}} a^3 \sum_{\mathbf{y}} Z r_{\rm m} \langle P^a(y) O^a \rangle + {\rm O}(am, a^2)\,, \tag{9f}$$

having divided by $Z_A Z_S^0$ and employed $r_{\rm m} = \frac{Z_{\rm S}}{Z_{\rm S}^0}$ and $Z = \frac{Z_{\rm P}}{Z_{\rm A} Z_{\rm S}}$. Hence, the only unknown quantity left is $g_{\rm S}$; we already determined Z and $r_{\rm m}$ in [11] and $c_{\rm A}$ in [12]. Note that quark-line disconnected diagrams appear in some of the three-point functions as a consequence of the flavour singlet property of the Ward identity considered here. Our determinations of Z and $r_{\rm m}$ are based on flavour non-singlet Ward identities; thus no such disconnected diagrams entered there.

3. Numerical Setup

L/a	β	κ	#REP	$N_{\rm sep}$ [MDU]	$N_{\rm cnfg}$	$am^{\rm impr}$
12	3.4014	0.1368240	4	8	10466	0.00065(16)
16	3.5522	0.1371379	4	8	11992	0.000056(67)
20	3.6900	0.1371452	10	4	10000	0.000094(59)
24	3.8013	0.1370387	2	8	8000	−0.000008(35)
32	3.9764	0.1367450	2	4	10072	0.000011(14)

Table 1: Simulation parameters $L(=T)$, β, κ, the number of replica #REP and $N_{\rm sep}$, the number of molecular dynamics units, MDU, all configurations are separated by. The ensembles are labelled by their lattice extent i.e. L12, L16, L20, L24, L32, and were originally generated as part of another study [13, 14]; we have (approximately) doubled the statistics of the ensembles L12 and L16. For each ensemble we list the O(a) improved PCAC mass $am^{\rm impr}$ obtained by averaging over the local masses of the three central time slices.

We employ the tree-level Symanzik-improved gauge action with $N_{\rm f} = 3$ mass-degenerate O(a) improved Wilson fermions. For the corresponding improvement coefficient $c_{\rm sw}$ we use the non-perturbative determination of [15]. As for our earlier determination of Z and $r_{\rm m}$ [11] we impose

Schrödinger functional boundary conditions at the temporal boundaries of the lattice since this setup is well-suited for massless renormalisation schemes. All gauge field ensembles used in this study are summarised in table 1 and lie on a precisely tuned line of constant physics (LCP), defined by a fixed spatial and temporal extent of $L = T \approx 1$ fm and (nearly) massless quarks, see table 1. For the tuning, the gradient flow running coupling was kept constant, see [13, 14, 16]; the ensembles were originally generated as part of another study [13, 14] and we have (approximately) doubled the statistics of the ensembles L12 and L16. The LCP ensures that our estimates of $g_{\rm S}$ become smooth functions of the lattice spacing, higher-order ambiguities vanishing monotonically. For all ensembles we use one-loop boundary O(a) improvement for both the gauge and fermion fields (i.e. the appropriate $c_{\rm t}, \widetilde{c}_{\rm t}$ values). For full O(a) improvement of the Schrödinger functional correlation functions we additionally require the improvement coefficient $c_{\rm A}$, non-perturbatively known from [12]. Consequently, the quantity of interest, $g_{\rm S}$, is the only unknown quantity in our numerical calculations (based on eq. (10)) as we make use of our results for Z and $r_{\rm m}$ from [11].

Most of the needed correlation functions needed overlap with those already implemented and evaluated in [11]. Due to the now flavour singlet nature of the Ward identities, two additional types of correlation functions are relevant: we implement single propagator traces via stochastic estimators. To reduce the variance at moderate cost we combine frequency splitting, to treat intermediate modes, and a hopping parameter expansion, to treat the high modes, as proposed in [17]. We incorporate the necessary gluonic contributions in an `openQCD` based code [18], as anticipated below eq. (8), including all contributing rectangles and plaquettes symmetrically w.r.t. the site of the bilinear.

The Markov chain Monte Carlo sampling of the gauge field configurations suffers from critical slowing down of the topological charge for smaller lattice spacings. As in [11], we project the data to the trivial topological sector (as suggested in [19]) so that the insufficient sampling of all sectors is no longer relevant: Ward identities hold in one sector only as well, irrespective of the sector at hand. The statistical error analysis is carried out with `pyerrors`, a `python` implementation [20] of the Γ-method [21], combined with linear error propagation via automatic differentiation [22, 23].

4. Analysis

We write down the $g_{\rm S}$ Ward identity introduced in eq. (9) in terms of the Schrödinger functional correlation functions with explicit flavour indices i, j not summed over; note that the Wick contractions are not written out here. We obtain[1]

$$\left[f_{\rm AS}^{ij,\rm con}(t_2,y_0) - N_{\rm f} f_{\rm AS}^{ij,\rm disc}(t_2,y_0)\right] - \left[f_{\rm AS}^{ij,\rm con}(t_1,y_0) - N_{\rm f} f_{\rm AS}^{ij,\rm disc}(t_1,y_0)\right] \tag{10a}$$

$$+\left[f_{\rm A}^{ij}(t_2) - f_{\rm A}^{ij}(t_1)\right] N_{\rm f} f_{\langle \rm S\rangle}^{ii}(y_0) \tag{10b}$$

$$-g_{\rm S}\left\{2\left[f_{\rm AE}^{ij,\rm disc}(t_2,y_0) - f_{\rm AE}^{ij,\rm disc}(t_1,y_0)\right] - 2[f_{\rm A}^{ij}(t_2) - f_{\rm A}^{ij}(t_1)] f_{\langle \rm E\rangle}(y_0)\right\} \tag{10c}$$

$$+c_{\rm A}\left\{a\partial_{t_2}\left[f_{\rm PS}^{ij,\rm con}(t_2,y_0) - N_{\rm f} f_{\rm PS}^{ij,\rm disc}(t_2,y_0)\right] - a\partial_{t_1}\left[f_{\rm PS}^{ij,\rm con}(t_1,y_0) - N_{\rm f} f_{\rm PS}^{ij,\rm disc}(t_1,y_0)\right]\right. \tag{10d}$$

[1]Note that we no longer use the conventions from [1] but those employed in [7] because of the way correlation functions are defined in our `openQCD` based codes. In the former a hermitian $F_{\mu\nu}$ is used while an anti-hermitian definition is utilised in the latter case. We still label the improvement parameter of the flavour singlet density by $g_{\rm S}$ from [1], as before, by replacing $d_{\rm S}$, used in the latter convention [7], by $-gs$ as $g_{\rm S} = -d_{\rm S}$.

$$+\left[a\partial_{t_2} f_{\mathrm{P}}^{ij}(t_2) - a\partial_{t_1} f_{\mathrm{P}}^{ij}(t_1)\right] N_{\mathrm{f}} f_{\langle \mathrm{S}\rangle}^{ii}(y_0)\Big\} \tag{10e}$$

$$-2am\left\{\left[\tilde{f}_{\mathrm{PS}}^{ij,\mathrm{con}}(t_1,t_2,y_0) - N_{\mathrm{f}}\tilde{f}_{\mathrm{PS}}^{ij,\mathrm{disc}}(t_1,t_2,y_0)\right] + \tilde{f}_{\mathrm{P}}^{ij}(t_1,t_2) N_{\mathrm{f}} f_{\langle \mathrm{S}\rangle}^{ii}(y_0)\right. \tag{10f}$$

$$\left. - g_{\mathrm{S}} \cdot 2\left[\tilde{f}_{\mathrm{PE}}^{ij,\mathrm{disc}}(t_1,t_2,y_0) - \tilde{f}_{\mathrm{P}}^{ij}(t_1,t_2) f_{\langle \mathrm{E}\rangle}(y_0)\right]\right\} \tag{10g}$$

$$= -2Z r_{\mathrm{m}} f_{\mathrm{P}}^{ij}(y_0) + \mathrm{O}(am, a^2)\,, \tag{10h}$$

where 'disc' refers to quark-line disconnected contributions. In this notation the explicit N_{f} dependence, a consequence of the flavour singlet nature of the identity, becomes apparent: Clearly, only the quark-line disconnected diagrams are multiplied by N_{f}, in particular those that involve S^0 and not those that are purely gluonic ($f_{\langle \mathrm{E}\rangle}$). Thus, regarding the Wick contractions this can be understood as an additional quark loop for each additional quark flavour. Except for the quark-line and gluonic disconnected contributions, this flavour singlet identity is not that different from the flavour non-singlet case considered in [11] for the determination of Z: The connected correlation functions are the same, i.e. with the same Wick contractions, disregarding different prefactors which result from the different flavour structures. Thus the definitions of the above correlation functions can be found in the appendices of [11]. Note that 'con' superscripts were not used then because of the lack of disconnected contributions. We list the additional correlation functions needed here:

$$f_{\mathrm{AS}}^{ij,\mathrm{disc}}(x_0,y_0) = -\frac{1}{2}\frac{a^{12}}{L^3}\sum_{\mathbf{x},\mathbf{y},\mathbf{u},\mathbf{v}}\left\langle\left\langle\bar{\psi}_i(x)\gamma_0\gamma_5\psi_j(x)\cdot\bar{\zeta}_j(\mathbf{u})\gamma_5\zeta_i(\mathbf{v})\right\rangle_{\mathrm{F}}\cdot\left\langle\bar{\psi}_j(y)\mathbb{1}\psi_j(y)\right\rangle_{\mathrm{F}}\right\rangle_G . \tag{11}$$

Substituting $\gamma_0\gamma_5$ by γ_5 we define $f_{\mathrm{PS}}^{ij,\mathrm{con}}(x_0,y_0)$ and $f_{\mathrm{PS}}^{ij,\mathrm{disc}}(x_0,y_0)$ analogously. For the same analysis, we also need to establish

$$f_{\mathrm{AE}}^{ij,\mathrm{disc}}(x_0,y_0) = -\frac{1}{2}\frac{a^9}{L^3}\sum_{\mathbf{x},\mathbf{y},\mathbf{u},\mathbf{v}}\left\langle\left\langle\bar{\psi}_i(x)\gamma_0\gamma_5\psi_j(x)\cdot\bar{\zeta}_j(\mathbf{u})\gamma_5\zeta_i(\mathbf{v})\right\rangle_{\mathrm{F}}\cdot\left\langle E(y)\right\rangle_{\mathrm{F}}\right\rangle_G . \tag{12}$$

and the purely gluonic case of $f_{\langle \mathrm{E}\rangle}(y_0) = a^4/2\sum_{\mathbf{y}}\langle\widetilde{\mathrm{Tr}}[FF](y)\rangle_G$. The correlation functions $\tilde{f}_{\mathrm{PS}}^{ij,\mathrm{con}}(t_1,t_2,y_0)$, $\tilde{f}_{\mathrm{PS}}^{ij,\mathrm{disc}}(t_1,t_2,y_0)$ and $\tilde{f}_{\mathrm{PE}}^{ij,\mathrm{disc}}(t_1,t_2,y_0)$ are defined by

$$\tilde{f}^{ij}(t_1,t_2,y_0) = \sum_{x_0=t_1}^{t_2}\omega(x_0) f^{ij}(x_0,y_0) \quad \text{where} \quad \omega(x_0) = \begin{cases}\frac{1}{2}, & \text{for } x_0 = t_1, t_2\\ 1, & \text{otherwise}\end{cases} \tag{13}$$

setting, e.g. $f^{ij}(x_0,y_0) = f_{\mathrm{PS}}^{ij,\mathrm{con}}(t_1,t_2,y_0)$ for $\tilde{f}_{\mathrm{PS}}^{ij,\mathrm{con}}(t_1,t_2,y_0)$. The single propagator trace contributing is defined by $f_{\langle \mathrm{S}\rangle}^{ii}(y_0) = a^3\sum_{\mathbf{y}}\left\langle\bar{\psi}_i(y)\mathbb{1}\psi_i(y)\right\rangle$.

We evaluate the Ward identity for $N_{\mathrm{f}} = 3$ on the ensembles summed up in table 1: by working close to the chiral limit with (nearly) vanishing quark masses (see table 1), O(am) effects may be safely neglected and the Ward identity becomes valid up to O(a^2) cut-off effects. In [11] we found that for our Z Ward identity the term above proportional to the current quark mass m, which can in principle be discarded in the chiral limit, still stabilises the chiral extrapolation (also found in refs. [24–27] previously). Thus we prefer to keep it here too (even though we do not perform chiral extrapolations here but extract the Ward identity in the (nearly) chiral limit). We evaluate the operators P^a and S^0 at $t_1 \approx T/3$ and $t_2 \approx 2T/3$ (labelled by $T/3$) respectively, or alternatively at $t_1 \approx T/4$ and $t_2 \approx 3T/4$ (labelled by $T/4$). In practice, we round t_1 and t_2 to the nearest integer

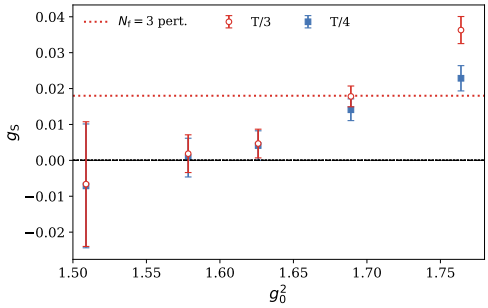

Figure 1: g_S results obtained via eq. (10) for $N_f = 3$ using our Z and r_m interpolation formulas from [11] to construct the Zr_m values at the given couplings needed. The perturbative prediction from eq. (3) (dashed red line) cannot be directly compared to the g_S data points, see text below. The time interval $[t_1, t_2]$ (in eq. (10)) is set to $[T/4, 3T/4]$ (labelled by T/4) or $[T/3, 2T/3]$ (labelled by T/3) as shown by different colours.

when $T/3$ and $T/4$ are not integers. We made the same choices previously for the determination of Z in [11]. We extract the necessary PCAC mass plateaus by averaging over the local mass results of the three central time slices, see table 1 for the results at each coupling.

Putting everything together and solving the Ward identity for g_S, we obtain g_S estimates at five lattice spacings and for two choices of the time interval labelled $T/3$ and $T/4$, shown in fig. 1. We find that both g_S estimates approach zero for small couplings and are even compatible with zero within their respective 1σ-errors at the two smallest couplings available; g_S at the next higher coupling is close to zero as well. We also display the prediction from perturbation theory. Note that this perturbative prediction needs to be treated with caution in the present context since it is derived by applying $b_g = 2g_0^2 g_S$ to the perturbative prediction of b_g, cf. eq. (3). As we will discuss in the next section the g_S estimates here cannot be used in this relation to obtain b_g: for eq. (1) to hold our non-perturbative definition of g_S through eq. (10) needs an additional term, which is merely an O(a) ambiguity for g_S. Therefore, the perturbative prediction can only give us an idea of the order of magnitude of g_S; as can be inferred from fig. 1 our g_S estimates differ from the perturbative prediction but the order of magnitude agrees well.

5. Conclusion and Outlook

We were able to determine non-perturbative estimates for g_S for the first time. They were determined employing the tree-level Symanzik-improved gauge action with $N_f = 3$ mass-degenerate O(a) improved Wilson fermions and lie in the range of the CLS couplings, $g_0^2 \in [1.5, 1.77]$.

As to be able to make use of the g_S–b_g relation and extract b_g estimates from our g_S estimates additional steps are necessary. As derived in appendix A of [7] via gradient flow observables the derivative of the full lattice action w.r.t. the coupling g_0^2 enters the derivation of the g_S–b_g relation. In the action used here not only the gauge action depends on the coupling but also the O(a) improved fermionic part of the action, through the improvement coefficient $c_{sw}(g_0^2)$. This introduces an additional term $\propto c_{sw}(g_0^2)$ in the derivation which was possibly overlooked in the original publication [1]. For the g_S–b_g relation to be preserved in the O(a) improved theory, this term must also be taken into account in the choice of discretisation used for $\mathrm{Tr}(F_{\mu\nu}F_{\mu\nu})(x)$ in the

improvement of the flavour singlet density, introduced in eq. (8). This amounts to [7]

$$\widetilde{\mathrm{Tr}}[F_{\mu\nu}(x)F_{\mu\nu}(x)] \to \left(\{\widetilde{\mathrm{Tr}}[FF](x)\}^{S_\mathrm{g}} + ag_0^2 \times \frac{\partial c_\mathrm{sw}(g_0^2)}{\partial g_0^2}\frac{\mathrm{i}}{2}O^{\mathrm{clover}}(x)\right) \tag{14}$$

where $\{\widetilde{\mathrm{Tr}}[FF](x)\}^{S_\mathrm{g}}$ is the discretisation only based on the gauge action, used to determine g_S here. The additional term is the derivative w.r.t. g_0^2 of the fermionic part of the full O(a) improved action used here, introducing a dependence on the clover term.

Therefore, so that the g_S estimates can be related to b_g via $b_\mathrm{g} = 2g_0^2 g_\mathrm{S}$ the additional, clover term like expression needs to be included too, i.e. the Ward identity from eq. (9) needs to be reevaluated with $\{\widetilde{\mathrm{Tr}}[FF](x)\}^{S_\mathrm{g}}$ replaced by eq. (14). More precisely, we add to the l.h.s. of eq. (10) two terms of the form (where 'C' stands for the insertion of the clover term like expression)

$$-g_\mathrm{S}\left\{\left[f_\mathrm{AC}^{ij,\mathrm{con}(t_2,y_0)} - N_\mathrm{f} f_\mathrm{AC}^{ij,\mathrm{disc}}(t_2,y_0)\right] - \left[f_\mathrm{AC}^{ij,\mathrm{con}}(t_1,y_0) - N_\mathrm{f} f_\mathrm{AC}^{ij,\mathrm{disc}}(t_1,y_0)\right]\right\}, \tag{15}$$

$$+2am\cdot g_\mathrm{S}\left\{\left[\tilde{f}_\mathrm{PC}^{ij,\mathrm{con}}(t_1,t_2,y_0) - N_\mathrm{f}\tilde{f}_\mathrm{PC}^{ij,\mathrm{disc}}(t_1,t_2,y_0)\right] + \tilde{f}_\mathrm{P}^{ij}(t_1,t_2)N_\mathrm{f} f_{\langle\mathrm{C}\rangle}^{ii}(y_0)\right\} \tag{16}$$

similar to eq. (10a) and eq. (10f), respectively, i.e. with the clover term like part from eq. (14) instead of S^0 and with an additional factor, namely g_S. Despite its gluonic component, $f_{\langle\mathrm{C}\rangle}(y_0)$ can be evaluated similarly to $f_{\langle\mathrm{S}\rangle}^{ii}(y_0)$ (cf. sect. 3) since the expectation value can be rearranged such that the same single propagator trace $S(x,x)$ appears,

$$f_{\langle\mathrm{C}\rangle}(x_0) \sim -\frac{a^3}{2}\sum_{\mathbf{x}}\left\langle S(x,x)_{\beta\alpha}^{ba}\left(\sigma_{\mu\nu}F_{\mu\nu}^{\mathrm{clover}}\right)_{\alpha\beta}^{ab}(x)\right\rangle = -\frac{a^3}{2}\sum_{\mathbf{x}}\left\langle \eta^k, \left(\sigma_{\mu\nu}F_{\mu\nu}^{\mathrm{clover}}\right)^{kl} D^{-1}\eta^l\right\rangle \tag{17}$$

where $\eta^k(\eta^l)$ is the $k(l)$th (colour, Dirac) component of a stochastic noise source, $k(l) = 1,\ldots,12$ and a, b denote colour and α,β Dirac indices. The term $\left(\sigma_{\mu\nu}F_{\mu\nu}^{\mathrm{clover}}\right)$ is a 12×12 matrix (3×3 colour matrix times 4×4 Dirac matrix). In practice this clover Dirac-colour matrix is computed on every lattice point and multiplied by the stochastic estimator, which the inverse Dirac operator, D^{-1}, is applied to before. This implementation is the most challenging part and is currently being tested; the coding of the other additional diagrams is more straight forward. Once all these additional diagrams are implemented, we plan to redetermine g_S from the altered Ward identity. The new g_S estimates are expected to differ from the former in cut-off effects. We then plan to apply $b_\mathrm{g} = 2g_0^2 g_\mathrm{S}$ to extract non-perturbative b_g estimates in the range of the CLS couplings, $g_0^2 \in [1.5, 1.77]$. Ultimately, we then intend to fit $b_\mathrm{g}(g_0^2)$ as a smooth function of g_0^2 including the one-loop perturbative constraint from eq. (2) as to arrive at an interpolation formula. We plan to repeat the same procedure for the altered g_S using the perturbative constraint from eq. (3).

Acknowledgments

We thank Anastassios Vladikas for participating in this project in its early stages. We also thank Rainer Sommer and Stefan Sint for useful discussions. This work was supported by the U.S. Department of Energy contract DE-AC05-06OR23177, under which Jefferson Science Associates, LLC operates Jefferson Lab (P. L. J. P.) and by the Deutsche Forschungsgemeinschaft (DFG) through the Research Training Group "GRK 2149: Strong and Weak Interactions – from Hadrons to Dark Matter" (P. L. J. P., J. H., F. J.). Computations for this publication were performed on the HPC cluster PALMA II of the University of Münster.

References

[1] T. Bhattacharya, R. Gupta, W. Lee, S. R. Sharpe and J. M. Wu, *Improved bilinears in lattice QCD with non-degenerate quarks*, *Phys. Rev. D* **73** (2006) 034504 [hep-lat/0511014].

[2] Flavour Lattice Averaging Group (FLAG) collaboration, Y. Aoki et al., *FLAG Review 2021*, *Eur. Phys. J. C* **82** (2022) 869 [2111.09849].

[3] Flavour Lattice Averaging Group (FLAG) collaboration, Y. Aoki et al., *FLAG Review 2024*, 2411.04268.

[4] A. Agadjanov, D. Djukanovic, G. von Hippel, H. B. Meyer, K. Ottnad and H. Wittig, *Nucleon Sigma Terms with $N_f = 2 + 1$ Flavors of O(a)-Improved Wilson Fermions*, *Phys. Rev. Lett.* **131** (2023) 261902 [2303.08741].

[5] M. Lüscher, S. Sint, R. Sommer and P. Weisz, *Chiral symmetry and* O(a) *improvement in lattice QCD*, *Nucl. Phys. B* **478** (1996) 365 [hep-lat/9605038].

[6] S. Sint and P. Weisz, *Further results on O(a) improved lattice QCD to one loop order of perturbation theory*, *Nucl. Phys. B* **502** (1997) 251 [hep-lat/9704001].

[7] ALPHA collaboration, M. Dalla Brida, R. Höllwieser, F. Knechtli, T. Korzec, S. Sint and R. Sommer, *Heavy Wilson quarks and O(a) improvement: nonperturbative results for b_g*, *JHEP* **01** (2024) 188 [2401.00216].

[8] ALPHA collaboration, M. Dalla Brida, R. Höllwieser, F. Knechtli, T. Korzec, A. Nada, A. Ramos, S. Sint and R. Sommer, *Determination of $\alpha_s(m_Z)$ by the non-perturbative decoupling method*, *Eur. Phys. J. C* **82** (2022) 1092 [2209.14204].

[9] RQCD collaboration, G. S. Bali, S. Collins, P. Georg, D. Jenkins, P. Korcyl, A. Schäfer, E. E. Scholz, J. Simeth, W. Söldner and S. Weishäupl, *Scale setting and the light baryon spectrum in $N_f = 2 + 1$ QCD with Wilson fermions*, *JHEP* **05** (2023) 035 [2211.03744].

[10] S. Sint, *Renormalization of the iso-singlet scalar density in lattice QCD with Wilson quarks*, *Nucl. Phys. B Proc. Suppl.* **73** (1999) 282.

[11] J. Heitger, F. Joswig, P. L. J. Petrak and A. Vladikas, *Ratio of flavour non-singlet and singlet scalar density renormalisation parameters in $N_f = 3$ QCD with Wilson quarks*, *Eur. Phys. J. C* **81** (2021) 606 [2101.10969], [Erratum: Eur. Phys. J. C 82, 104 (2022)].

[12] J. Bulava, M. Della Morte, J. Heitger and C. Wittemeier, *Non-perturbative improvement of the axial current in $N_f = 3$ lattice QCD with Wilson fermions and tree-level improved gauge action*, *Nucl. Phys. B* **896** (2015) 555 [1502.04999].

[13] P. Fritzsch, J. Heitger and S. Kuberski, *$O(a)$ improved quark mass renormalization for a non-perturbative matching of HQET to three-flavor QCD*, *PoS* **LATTICE2018** (2018) 218 [1811.02591].

[14] A. Conigli, J. Frison, P. Fritzsch, A. Gérardin, J. Heitger, G. Herdoiza, S. Kuberski, C. Pena, H. Simma and R. Sommer, *m_b and $f_{B^{(*)}}$ in 2 + 1 flavour QCD from a combination of continuum limit static and relativistic results*, *PoS* **LATTICE2023** (2024) 237 [2312.10017].

[15] J. Bulava and S. Schaefer, *Improvement of $N_f = 3$ lattice QCD with Wilson fermions and tree-level improved gauge action*, *Nucl. Phys. B* **874** (2013) 188 [1304.7093].

[16] ALPHA collaboration, M. Dalla Brida, P. Fritzsch, T. Korzec, A. Ramos, S. Sint and R. Sommer, *Slow running of the Gradient Flow coupling from 200 MeV to 4 GeV in $N_f = 3$ QCD*, *Phys. Rev. D* **95** (2017) 014507 [1607.06423].

[17] L. Giusti, T. Harris, A. Nada and S. Schaefer, *Frequency-splitting estimators of single-propagator traces*, *Eur. Phys. J. C* **79** (2019) 586 [1903.10447].

[18] M. Lüscher and S. Schaefer. http://luscher.web.cern.ch/luscher/openQCD.

[19] P. Fritzsch, A. Ramos and F. Stollenwerk, *Critical slowing down and the gradient flow coupling in the Schrödinger functional*, *PoS* **Lattice2013** (2014) 461 [1311.7304].

[20] F. Joswig, S. Kuberski, J. T. Kuhlmann and J. Neuendorf, *pyerrors: A python framework for error analysis of Monte Carlo data*, *Comput. Phys. Commun.* **288** (2023) 108750 [2209.14371].

[21] U. Wolff, *Monte Carlo errors with less errors*, *Comput. Phys. Commun.* **156** (2004) 143 [hep-lat/0306017], [Erratum: Comput. Phys. Commun. 176, 383 (2007)].

[22] A. Ramos, *Automatic differentiation for error analysis of Monte Carlo data*, *Comput. Phys. Commun.* **238** (2019) 19 [1809.01289].

[23] ALPHA collaboration, S. Schaefer, R. Sommer and F. Virotta, *Critical slowing down and error analysis in lattice QCD simulations*, *Nucl. Phys. B* **845** (2011) 93 [1009.5228].

[24] J. Bulava, M. Della Morte, J. Heitger and C. Wittemeier, *Nonperturbative renormalization of the axial current in $N_f = 3$ lattice QCD with Wilson fermions and a tree-level improved gauge action*, *Phys. Rev. D* **93** (2016) 114513 [1604.05827].

[25] J. Heitger, F. Joswig and A. Vladikas, *Ward identity determination of Z_S/Z_P for $N_f = 3$ lattice QCD in a Schrödinger functional setup*, *Eur. Phys. J. C* **80** (2020) 765 [2005.01352].

[26] ALPHA collaboration, J. Heitger and F. Joswig, *The renormalised* O(a) *improved vector current in three-flavour lattice QCD with Wilson quarks*, *Eur. Phys. J. C* **81** (2021) 254 [2010.09539].

[27] L. Chimirri, P. Fritzsch, J. Heitger, F. Joswig, M. Panero, C. Pena and D. Preti, *Non-perturbative renormalisation and improvement of non-singlet tensor currents in $N_f = 3$ QCD*, *JHEP* **07** (2024) 089 [2309.04314].